water

MDPI

Article

Hydrogeological Hazards in Open Pit Coal Mines–Investigating Triggering Mechanisms by Validating the European Ground Motion Service Product with Ground Truth Data

Ploutarchos Tzampoglou [1,2,*] and Constantinos Loupasakis [1]

[1] Laboratory of Engineering Geology and Hydrogeology, Department of Geological Sciences, School of Mining and Metallurgical Engineering, National Technical University of Athens, 15780 Athens, Greece; cloupasakis@metal.ntua.gr
[2] Department of Civil & Environmental Engineering, University of Cyprus, Nicosia 1678, Cyprus
* Correspondence: tzampoglou.ploutarchos@ucy.ac.cy

Abstract: This research focuses on the investigation of hydrogeological hazards in open pit coal mines. The study area is the Amyntaio sub-basin area, located in West Macedonia prefecture, Greece. A major part of the SE of this area is occupied by the Amyntaio open pit coal mine. In recent decades, the Amyntaio basin's aquifer has been overexploited both by dewatering wells of the open pit coal mine and irrigation wells, triggering extensive land subsidence in an area that extends 3 km around the mine. Additionally, one of the biggest mining landslides worldwide occurred on the South-West slopes of the open pit on 10 June 2017. The current study investigates the land subsidence phenomenon and the landslide, highlighting the influence and the interaction of their causal factors which were strongly affected by the groundwater management. To estimate ground surface movement, Earth Observation data from the European Ground Motion Service, of the Copernicus European Union's Earth observation program, were used for the period 1 January 2016–31 December 2020. The geologic, geotechnical and hydrogeologic data coming from the extensive ground truth survey have been incorporated with the Earth Observation data, highlighting the opposing mechanisms of the interacting geohazards.

Keywords: mining landslide; land subsidence; amyntaio basin; mining geohazards; ground water management; Copernicus; land monitoring

Citation: Tzampoglou, P.; Loupasakis, C. Hydrogeological Hazards in Open Pit Coal Mines–Investigating Triggering Mechanisms by Validating the European Ground Motion Service Product with Ground Truth Data. *Water* **2023**, *15*, 1474. https://doi.org/10.3390/w15081474

Academic Editor: Neil McIntyre

Received: 5 January 2023
Revised: 5 April 2023
Accepted: 6 April 2023
Published: 10 April 2023

1. Introduction

Anthropogenic activities, such as mining, significantly affect the natural environment [1], causing various types of hazards. The most common geohazards are land subsidence and landslides; these catastrophic events can occur during mining as well as in the post-mining period (in cases where appropriate mitigation measures are not taken) and can be triggered by a range of hydrologic, geologic, and tectonic factors. Specifically, 132 different cases of slope failures have been documented worldwide since 1960 [2], causing hundreds of deaths and massive economic damage. Key examples include the Bingham Canyon Mine landslide in Utah, USA, in which two landslides displaced around 145 million tons of geomaterial on 10 Arpil 2013 [3–6], and the Jade Mine landslide in the northern state of Kachin, Myanmar, in which over 170 people were killed [7]. In contrast, land subsidence slowly affects extensive areas around mines, causing mainly significant economic damage [8–12].

To date, many studies have been conducted to investigate the failure mechanisms triggering natural hazards such as landslides [13], land subsidence [14,15], floods [16,17], and seasonal ground movement due to swelling formations [18] using state of the art Earth Observation technologies. The use of Synthetic Aperture Radar Interferometry satellite data (InSAR) combined with the geotechnical research helps to obtain new insights into

the failure mechanisms of the geohazards. Furthermore, it can contribute significantly to estimating the main causal factors that play an active role in the occurrence of the geohazard. Thus, it can give the opportunity to take all the necessary measures for the mitigation of the catastrophic events.

The study area in this work is the Amyntaio sub-basin, which is located in the West Macedonia prefecture of Greece. A major part of the southeast of this area is occupied by the Amyntaio open pit coal mine. A 220 m deep coal mine that operated between 1989 and 2020, with 179 million tons of lignite production and 1595 million m^3 of total excavations.

There are four lakes and ten villages within the Amyntaio basin, and the basin's agricultural area exceeds 200 km^2. In recent decades, an extensive groundwater level drop has been recorded due to the overpumping of the aquifer, both for protecting the open pit coal mine's slopes (i.e., draining wells) and providing for the irrigation needs of the area's agricultural activity. Specifically, the groundwater level drawdown between May 1992 and May 2015 reaches 70 m near the mine, extending northwest to the village of Valtonera and west to Anargiroi village [19–23]. The drop in the groundwater level, combined with the area's general geotectonic setting, triggered extensive land subsidence in an area extending up to 2 km around the mine, causing damage to villages and infrastructure since 2002. Additionally, one of the world's largest mining landslides took place on the South-West slopes of the open pit mine on 10 June 2017. Based on previous studies, the landslide mass involved in this event was 80 million m^3 [24]. A timely prediction of this event allowed precautionary measures (such as stopping work inside the mine) to be taken and, therefore, loss of human life was avoided.

Aiming to further study the mechanisms of the catastrophic events that took place at the perimeter of the Amyntaio open pit coal mine, this study employs InSAR data from the European Ground Motion Service (EGMS) product covering the period 2016–2021. The EGMS provides reliable information regarding natural and anthropogenic ground motion over the Copernicus Participating States and across national borders, with millimeter accuracy [25–29].

The motivation of this study is to combine the ground truth datasets acquired for the study of the mining geohazards, namely land subsidence and landslide, with the EGMS InSAR data set, aiming to cross-verify their outcomes. The main objectives of the study are to (a) estimate the spatial distribution of the vertical deformation due to land subsidence and landslide by evaluating the EGMS InSAR datasets; (b) correlate the above data with the data obtain thought the geotechnical research highlighting opposite driving failures mechanisms and main causal factors and (c) estimate the interaction between these two catastrophic events.

The comparison of the ground truth survey data (that have been acquired for more than 15 years since 2005) with the INSAR datasets, provides an excellent case study to demonstrate the reliability and value of the EGMS product. The understanding of the failure mechanism of land subsidence and landslide as well the estimation of their interaction can help local and regional authorities to understand the arising risks. This knowledge will enable them to take appropriate mitigation measures to ensure the future safe landplaning development.

2. Study Area

2.1. Geologic, and Geotechnical Setting

The study area forms part of the Kozani–Amyntaio–Ptolemaida–Florina basin and belongs to the Pelagonian geotectonic zone. The area consists of a Paleozoic and Mesozoic crystalline schist bedrock covered by Neogene and Quaternary deposits. Based on previous geotechnical studies [23,30–32], some useful insights can be gained relating to the geotechnical behavior of the formations developed in the study area. In detail, the study area's geological formations are as follows (Figure 1).

Recent alluvial deposits: including lacustrine and peat deposits. They obtain high to extremely high compressibility index (Cc) values of up to 0.187 and 1.707, respectively.

Despite their high compressibility index, these units occur superficially and, therefore, are unlikely to be significantly affected by changes in groundwater levels; thus, they likely do not play a major role in driving land subsidence due to overexploitation of the aquifer. However, these units exhibit land subsidence driven by oxidation as a result of their high organic content levels.

Anargiroi Formation: Quaternary formation comprising of silty–clayey sands and red clays with coarse-grained intercalations. This unit has high strength values, consistent with its soil grain distribution; its Cc value, which reaches 0.133 for the clay intercalations, is likely due to the presence of small amounts of swelling clay minerals. This formation occurs in hilly areas of the study region's lowlands, at heights above the aquifers' phreatic head. Thus, it is not directly affected by groundwater head variations and does not contribute to or interact with land subsidence phenomena.

Perdikas formation: Quaternary formation divided into sandy silty clay (65–75%), organic silty clay (10–20%), and coarse-grained (10–20%) layers with some organic silty–clayey intercalations in the upper part. This unit mainly occurs under the recent deposits across the majority of the basin. In terms of its geotechnical data, the Perdikas formation shows high Cc values due to the significant montmorillonite content, which reach 0.16 for the silty–clayey sand, 0.27 for the sandy silty clay, and 0.99 for the organic silty clay horizons. Therefore, this formation, as a result of its composition (around 65–75% clayey horizons) and its geotechnical setting, is prone to vertical deformation in areas where fluctuation of the aquifer occurs.

Proastio Formation: lower Quaternary formation consisting of sandy coarse-grained horizons with red silty–clayey sands, clays, and organic layers [33]. It can be separated into two distinct parts; the upper part consists of more than 80% coarse-grained material and the lower part contains over 30% silty clay layers. The average Cc values are 0.16 for the silty–clayey sands, 0.18 for the organic layers, and 0.16 for the sandy silty clay layers. Due to the minor contribution of the fine-grained layers in the stratigraphy of the Proastio formation, their impact on the overall land subsidence is considered insignificant.

The Neogene formations underlie the Proastio formation. They are separated into two series: (a) the lignite-bearing Ptolemaida formation (Amyntaio and Ptolemaida lignite deposits), which consists mainly of gray silty clays and clayey marls [34,35], and (b) the lignite-bearing Komnina formation (Vegora and Komnina lignite deposits), which consists of sand and clay layers with intercalations of xylite [35] and sandstones. These formations are over-consolidated and impermeable, occurring beneath the base of the aquifer. Thus, they are not considered prone to consolidation, even if the active stresses change. However, it should be stressed that throughout this formation, bedding-parallel shear zones with reduced shear strength values occur [36]. These zones are highly likely to contribute to the formation of failure planes along the working slopes. Therefore, although this formation is not susceptible to land subsidence, it is susceptible to landslide failures.

Alpine–pre-Alpine formations: these formations are divided into: (a) Paleozoic metamorphic rocks (gneiss and schists) and (b) Triassic–Lower Jurassic carbonate rocks (crystalline limestones and marbles) [37,38]. They mainly occur in the west of the basin.

The faults in the Amyntaio sub-basin can be separated into two groups [39–42]. The first, trending NW–SE, affects only the Alpine–pre-Alpine formations, and the second, trending NE–SW, extends up to the Quaternary deposits. Three active tectonic structures with NE-SW directions [43] occur in the Amyntaio basin (Figure 1): (a) the Petron–Xino Nero–Aetos fault (Fpxa) in the northwest; (b) the Anargiroi fault (Fang) in the south, and (c) the Vegoritida fault (Fveg) on the east to northeast side of the basin.

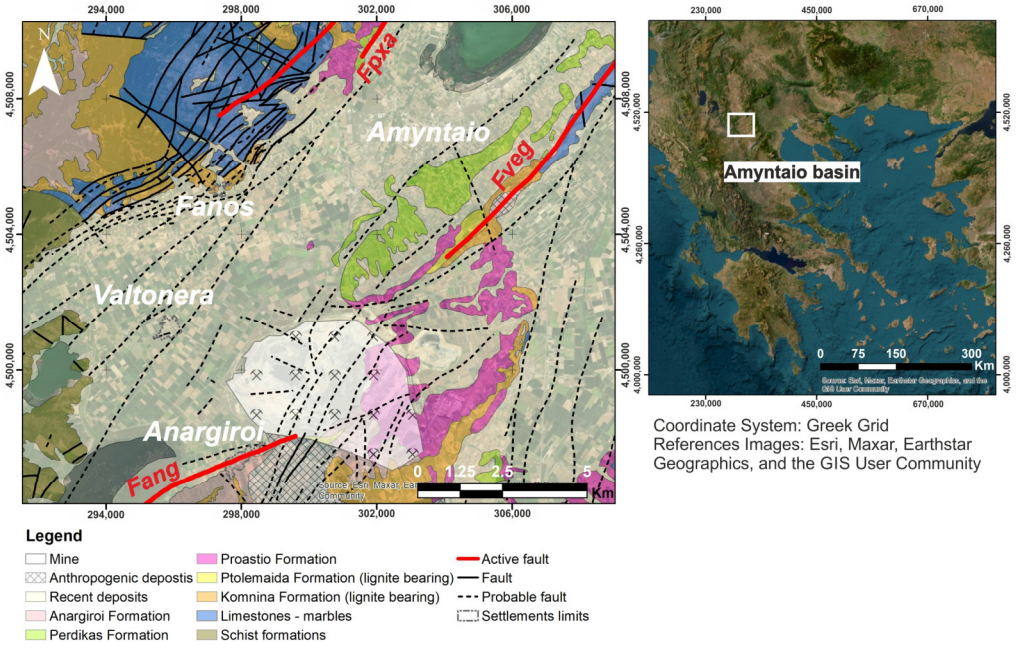

Figure 1. Geological map of the Amyntaio basin. The three active tectonic lines identified in the Amyntaio basin are clearly indicated.

2.2. Hydrogeologic Setting

Two aquifer systems can be identified in the Amyntaio sub-basin. The first one constitutes a karstic aquifer system within the Alpine–pre-Alpine bedrock formations, while the second one is developed in the Quaternary formations.

The piezometric head of the karstic aquifer system exceeds 100 m above the open pit bottom floor. Given that high piezometric loads were transferred on the slopes of the open pit mine in addition to the existence of bedding-parallel shear zones, negative slope stability conditions are expected [24]. Note that this aquifer does not affect the land subsidence phenomenon as it is not subjected to any kind of exploitation along its entire plane due to its depth, considering that it is completely isolated underneath the Neogene formations. The shallow semiconfined aquifer is recharged by both karstic water overflow, along the boundaries of the basin, and by filtration of surface water; its total depth does not exceed 120 m [44].

During recent decades, a significant level drop in this aquifer has been identified as a result of systematic overpumping both for protecting the open pit coal mine's slopes (i.e., draining wells) and providing for the irrigation needs of the area's agricultural activity. Considering the results of extensive field investigation measurement campaigns [20,45,46], some key conclusions concerning changes in the piezometric level are as follows (Figure 2A–E): according to the results of groundwater level measurements that were carried out at the end of the dry season (October 2014 and October 2015), the groundwater flow appears to occur toward the open pit mine, forming an extensive depression cone (Figure 2B,D). In addition, local dynamic depression cones of minor importance were observed in areas of agricultural activity. A similar groundwater flow trend was identified in data that were obtained from water level measurement campaigns during May 2015 and May 2016 (i.e., the end of the wet period). Therefore, currently the open pit along with the surrounding draining wells operate as an oversized (4 km wide) well, continuously draining a big part of the Amyntaio basin.

The evolution of the groundwater flow over time can be easily estimated by comparing equal-drawdown contour lines between May 1992–May 2015 [23] and May 1992–May 2016 [47]. Note that the data from May 1992 relate to the period before the operation of the open pit coal mine [48]. As shown in Figure 3A,B, the drawdown reaches 70 m near the working slopes of the mine and decreases with increasing distance away from the mine.

The depression cone extends to the west reaching to the villages of Valtonera and Anargiroi. On the contrary, as indicated in Figure 2A, before the operation of the mine, only a gentle groundwater flow from the west towards the east of the basin can be identified. It is clear that during the last three decades the operation of the mine and, secondarily, the increase of the agricultural activities radically changed the groundwater dynamics of the basin.

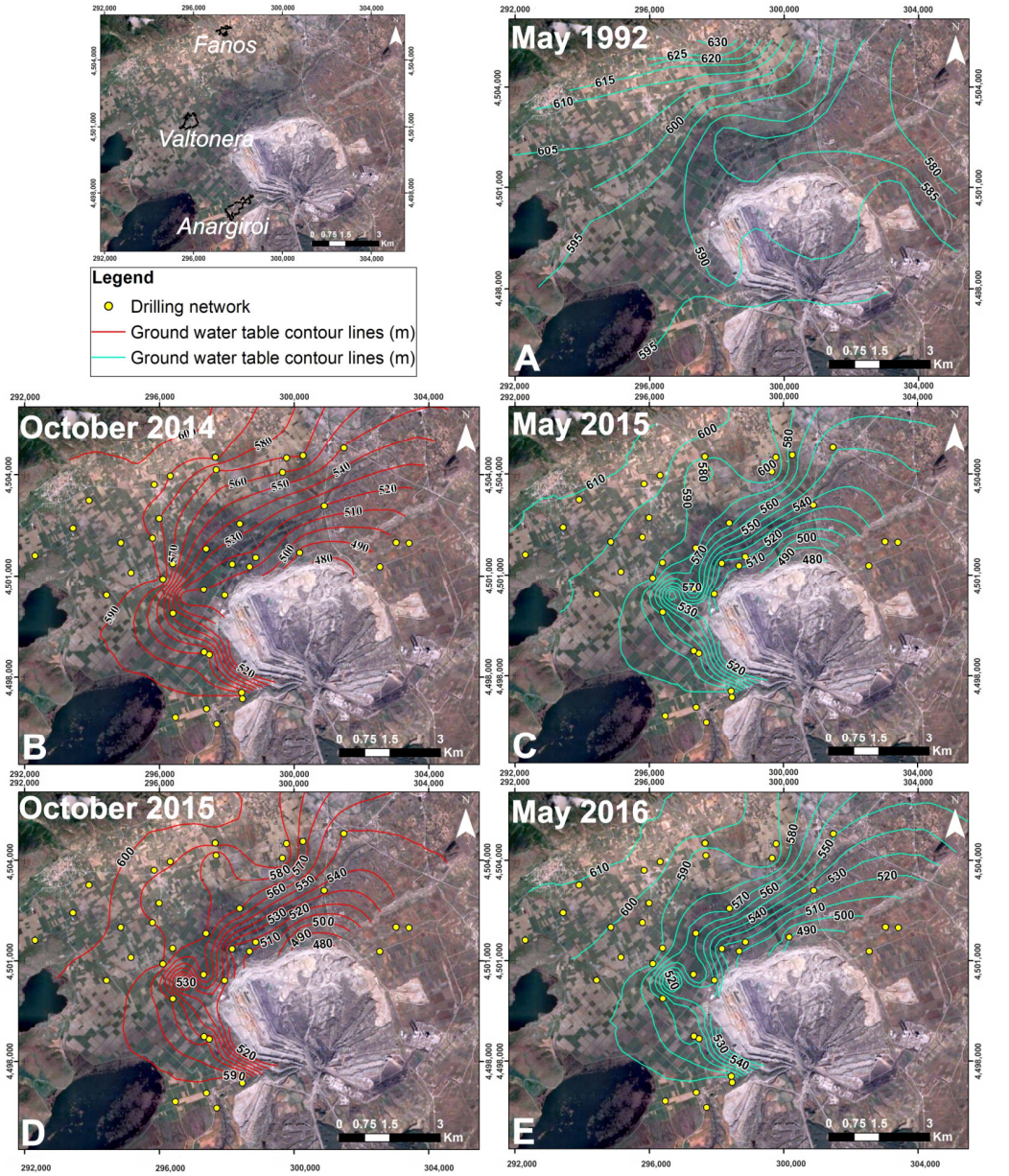

Figure 2. Ground water table contour lines based on the measurements carried out on: (**A**) May 1992 [48], (**B**) October 2014; (**C**) May 2015, (**D**) October 2016, and (**E**) May 2016.

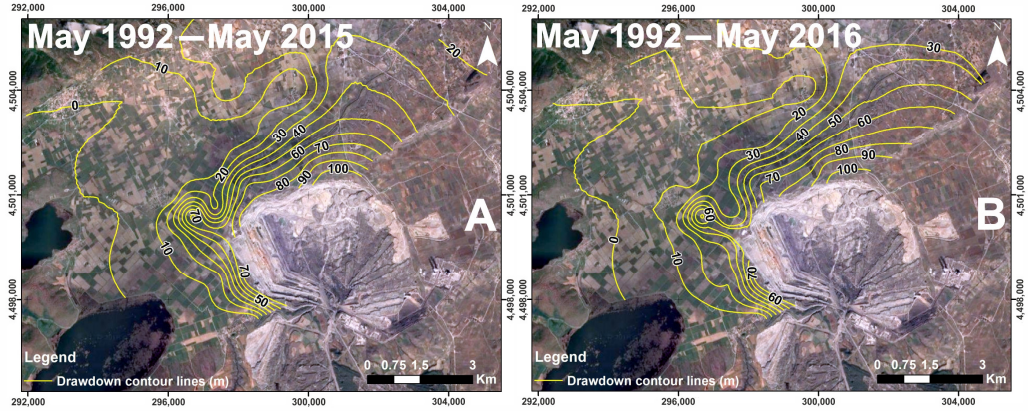

Figure 3. Equal drawdown contour lines between: (**A**) May 1992–May 2015 and (**B**) May 1992–May 2016.

3. Methodology for the Determination of the Catastrophic Events Driving Mechanism

Initially, all geological [34], tectonic [28,34,35,37,43], geotechnical [32] and hydrogeological [42] data, from previous studies, were collected and reevaluated during the 15 years long study, conducted by the authors of the current paper. New data sets have been added to the existing knowledge, including: (a) engineering geological mapping of the study area, (b) geotechnical laboratory tests' results from over 60 samples; (b) four ground water level measurements' campaigns (October 2014, May 2015, October 2015, May 2016) on a newly established network of over 40 wells and (c) detailed surface rapture mapping and infrastructure damage recording. All data sources taken into account are presented in the Supplementary Material (Table S1).

Aiming to validate the ground truth datasets as well as to identify the spatial distribution of deformation occurring in the villages surrounding the mine, data from the EGMS product were cross-validated with the above-described ground truth data sets. The EGMS is based on the multi-temporal interferometric analysis of Sentinel-1 radar images at full resolution. This technique allows for identifying reliable measurement points for which ground motion velocity values and time series of deformation are extracted [47]. The EGMS Ortho product provides purely vertical and purely east-west displacements over time with 100 m × 100 m output resolution cells. The data available for the studied site range from 5 January 2016 to 31 December 2021 [26], which includes the period of the landslide event that occurred on 10 June 2017.

The cross-validation of the Earth Observation data with the ground truth data sets provided a clear view on the driving mechanism of the land subsidence and landslide phenomena, highlighting their opposing triggering factors.

3.1. The Land Subsidence Mechanism

In 2001, Anargiroi village was affected by land subsidence. Until 2006, vertical deformation was recorded across the entire study area. To investigate the spatial distribution of surface ruptures in the Amyntaio basin, observations from previous studies were initially compiled [23,49–52]. Then, six field work campaigns were carried out, in which 15.5 km of surface ruptures were recorded (Figure 4). Most of these ruptures are oriented NW–SE and NE–SW, following the trends of the area's main fault lines. Thus, the tectonic faults acted as a pre-existing structural fabric that has controlled the orientation of later ruptures.

Three villages have been significantly affected by surface deformation (Anargiroi (Figure S1), Valtonera (Figure S2), and Fanos (Figure S3)) [23]. All these settlements share some common characteristics, namely (a) they are located in areas affected by groundwater level drawdown, (b) they are crossed by faults, and (c) they are underlain by the Perdikas formation.

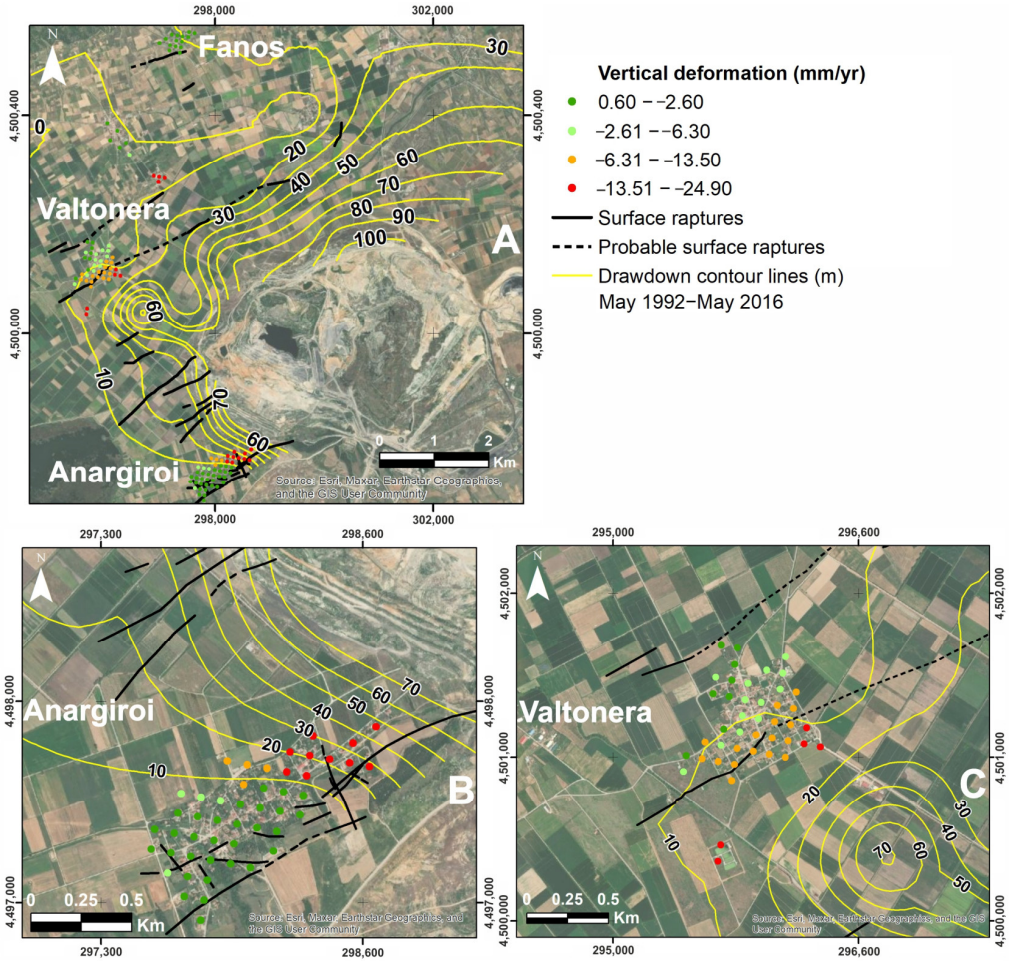

Figure 4. (**A**) Vertical deformations (mm/year) between 5 January 2016 and 31 December 2020 according to the InSAR data provided by Copernicus Land Monitoring Service [26] along with the recorded surfaces ruptures and the drawdown contour lines. (**B**,**C**) scale up view of the Anargiroi and Valtonera villages.

The vertical displacements of the surface ruptures appear to be proportional to the groundwater table drop and the distance from the mine. Specifically, the largest offsets (0.5 m to 1 m) are observed in areas near the mine where the groundwater withdrawal reaches 70 m. The differential displacements decrease with increasing distance from the mine and do not occur in areas where no water table level drop is recorded.

The correlation of the persistent scatterer (PS) point data obtained from the EGMS datasets (for the period between 5 January 2016 and 31 December 2020) with the recorded surface ruptures and drawdown contour lines for the period between May 1992 and May 2016 can be shown in Figure 4. Although the datasets do not refer to the exact same period, their correlation is applicable as the general hydrogeological conditions remain practically unchanged since 1992. The open pit keeps on operating as the main draining source while no extra irrigation wells have been drilled at the wider area. Evaluating the EGMS datasets, it is clear that the largest vertical displacement amplitudes, exceeding −20 mm/year, are observed to the northwest of Anargiroi village; the vertical deformation then decreases southeast of the village. This observation correlates closely with the recorded surface ruptures and drawdown contour lines, highlighting that land subsidence is still occurring in the study area.

Similar conclusions can be drawn from the PS points at Valtonera village. The observed water level drop in this area of around 10 to 20 m can trigger high-amplitude vertical displacements.

3.2. The Landslide Mechanism

On 10 June 2017, the largest recorded Greek mining landslide took place on the mining slopes of the Amyntaio open pit coal mine (Figure 5). According to estimates, the collapse mass reached 80 million m^3, extending over an area of 2 km in width and 2.2 km in length, while the foot of the landslide coincided with the lower point of the open pit mine at a depth of 210 m.

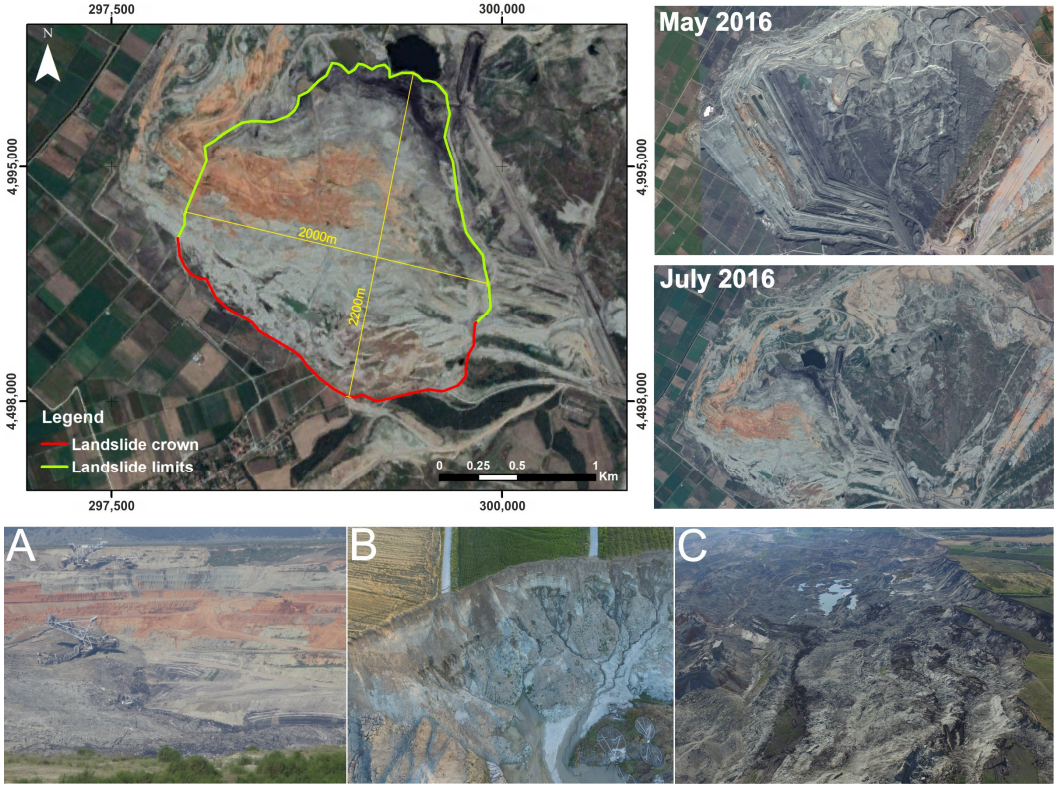

Figure 5. The spatial extent of the 10 June 2017 landslide at the Amyntaio mine, as shown by satellite imagery. Images obtained by Google Earth. (**A**–**C**) show oblique views of the landslide area. (**A**) one of the bucket wheel excavators buried inside the sliding mass; (**B**) panoramic view of the landslide scarp in front of the Anargyroi village; and (**C**) panoramic view of the landslide head looking towards East West.

The first signs of this failure were recorded some months before it occurred. In detail, eight months before the failure (November 2016), archaeological excavations, which were being carried out on the plain above the northwest side of the mine, were interrupted due to the occurrence of rapidly formed surface raptures caused by the increasing vertical deformation. In addition, five months before the failure (February 2017), deformation along the surface ruptures in the wider area of Anargiroi village began to increase. The timely recognition and prediction of the phenomenon allowed the evacuation of the open pit coal mine eight days before the failure, which contributed to avoiding the loss of lives.

Furthermore, the financial impacts of this landslide, which affected infrastructure both inside the mine and in the nearby area, were extremely large. Specifically, four bucket wheel excavators (weighing 500 to 1500 tons each), many small excavators, and several kilometers of conveyor were significantly damaged or buried inside the mine (Figure 5A). Additionally, 25 million tons of lignite were buried under the sliding mass, leading to further losses. Outside the open pit coal mine, the landslide caused enormous damage to the village of Anargiroi (Figure S4). In particular, the northwest part of Anargiroi village was severely damaged and permanently evacuated, the wastewater treatment plant collapsed into the pit (Figure 5B,C), and hundreds of meters of road network and

electricity and water supply infrastructure were destroyed (Figure 6A–E). Furthermore, an archaeological settlement of lacustrine Neolithic age, which was located at the western perimeter of the mine, disappeared as it collapsed into the open cast pit.

Figure 6. Spatial distribution of surface ruptures identified behind the crown of the 10 June 2017 landslide. (**A**,**B**) surface ruptures within the basin between Anargiroi and Valtonera village (the height of the scarp is approximately 1 m), (**C**,**D**) pre-existing surface ruptures caused by the land subsidence phenomenon that were intensified by the landslide event in the NW part of Anargiroi village, and (**E**) damage along the Anargyroi village road network.

To constrain the potential failure mechanism for this event, the three main triggering factors, tectonic activity, groundwater pore pressure, and slope geometry, were investigated. In terms of tectonic activity, according to the National Observatory of Greece's earthquake database [53], no earthquakes of magnitude 2.5 or above were recorded in the area surrounding the open pit in the five-month period preceding the landslides. Therefore, the area's tectonic activity is deemed to have not played a major active role in activating this particular landslide or in the associated pre-failure vertical deformation. Nonetheless, it should be stressed that the faults crossing the mine affected the formations occupying the working slopes of the mine, creating zones with reduced shear strength. In particular, the Vegoritida fault (F_{Veg}) defines the western boundary of the landslide while the Anargiri fault (F_{Ang}) crosses the crown and eastern boundary of the landslide. In addition, secondary parallel faults cross the site, affecting the geometry of the landslide mass. Thus, the tectonic structure of the study area can be characterized as a preparatory factor, but not a triggering causal factor, of the landslide on 10 June 2017.

In regard to the groundwater pore pressure, two aquifer systems occur in the study area. The aquifer system developed in the Quaternary formations has been systematically overexploited during recent decades, aiming to protect the mining slopes from failure. The volume of water pumped out from the aquifers, via the mine protection wells, was reduced over time as the subsurface consolidation resulted in compaction of the aquifers and a gradual reduction of their hydraulic conductivity. In detail, the protection wells

around the mine extracted 13 × 10^6 m^3/year of water in 2002, 9 × 10^6 m^3/year in 2009, and 3 × 10^6 m^3/year in 2016 [51]. Furthermore, the pumping activities directly adjacent to Anargiroi village, according to PPC [51], were essentially stopped in 2016, aiming to eliminate the deformation caused by overpumping at the nearby village. These two factors led to a steady increase in the water table between Anargiroi village and the mine, thereby significantly degrading the mechanical properties of the Quaternary deposits. This increase became visible after the occurrence of the landslide when water from the aquifer began gushing from the main scarp of the landslides (Figure 5B). In contrast, this did not occur along the northwestern parts of the main scarp where pumping activities were active at least since the slope failure (Figure 5C). Additionally, the karstic aquifer system created negative slope stability conditions by transferring piezometric load to the lower Neogene formations at the bottom of the mine.

The geometry of the working slopes was uneven and steep, negatively impacting their stability. The evaluation of all available satellite images of the mine illustrates that the two upper benches were excavated first in order to unload the slope. Subsequently, the excavation of the lower benches of the coal seams was prioritized to meet production needs. As a result, the excavation of the middle benches, occupied by the upper Neogene and lower Quaternary formations, was systematically neglected. Accordingly, the geometry of the working slopes was uneven, as the upper parts were more gently sloped and the lower parts steeper. This configuration, with a steeper base of the working slopes, raises significant issues concerning the overall safety factor.

Overall, the stratigraphy of the Neogene formations, including shear zones, the tectonic structure of the plain with faults crossing the mine, and the hydrogeologic setting with two aquifer systems interacting with the mine are considered to be the main preparatory factors for the studied landslide event. Respectively, the main triggering factors of this failure were: (a) the increase in the water table in the Quaternary formation aquifer due to selective reduction of pumping and (b) the steep geometry of the working slopes.

4. Results and Discussion

Based on the vertical and east-west displacement time series from PS points at the villages of Anargiroi, Valtonera, and Fanos, various insights can be gained into the spatial distribution of land subsidence and the impact of the landslide.

In regard to the Anargiroi village, the maximum vertical displacements occur in areas closer to the mine (Figures 4 and S1). This area is underlain by the highly compressible Perdikas Formation; in addition, the maximum groundwater dropdown values of the mine's depression cone occur in this area. As anticipated, the vertical displacement decreases (from NE to SW) in proportion to the groundwater level drop (Figures 4 and S1). In contrast, at the southwestern end of the village, only slight seasonal groundwater fluctuations appear to affect the displacements (A7).

Considering the vertical displacement time series, the village appears to be affected by a steadily decreasing deformation trend (i.e., decreasing land subsidence) during the period January 2016 to December 2020. This observation is directly linked with changes in pumping activities, which have practically stopped since 2016 (Figure 7), allowing partial recovery of the unconfined aquifer.

The abrupt fluctuations of PS points in both the vertical and east/west displacements that can be observed in the period around 10 June 2017, especially in the NE part of the village (i.e., A1, A2, A3, and A6), highlights the significant impact of the landslide. Furthermore, as clearly shown from the east–west horizontal displacement time series (Figure 7), the majority of the PSs around the NE part of the village display a steady eastward displacement trend, towards the open pit, after the landslide. The westward displacement trend identified at two PS points (A2 and A3) can be attributed to rotational movements of the structures that operated as reflectors for those two PSs. Thus, the present trends suggest that the studied site is slowly moving toward the abandoned 220 m deep open pit located only 180 m from the first houses of the village. Physical evidence of the

ongoing activity of the landslide can be obtained by the continuous deformations recorded at the damaged buildings located close to the open pit (Figure S7).

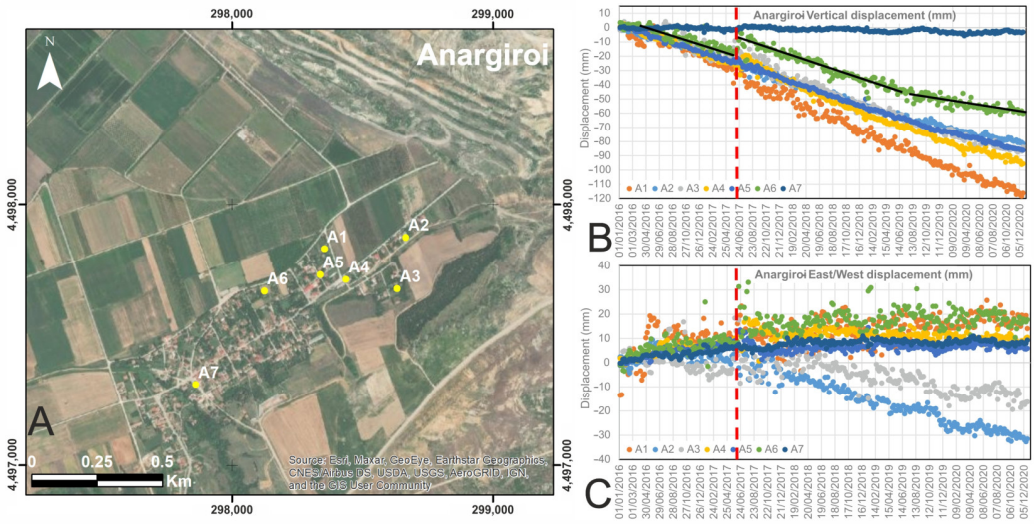

Figure 7. Spatial distribution of examined PS points (**A**) along with their displacement time series (**B**,**C**) at the village of Anargiroi. The dashed red line indicates the date of the mining landslide event. The trend lines added to the time series of point A6 indicate the variations of the land subsiding trend due to the draining activities before and after the occurrence of the landslide, as well as after the 2016 cessation of pumping from the wells located between the village and the open pit. Point A6 was selected as it clearly presents the disturbance caused by the landslide as well as the slight reduction of the deformations after the end of the end of the draining activities.

Consistent with the vertical displacement distribution identified at Anargiroi village, the deformation at Valtonera village increases toward the east, i.e., in areas closer to the mine (Figure 4). Similar to Anargiroi village, this area is also underlain by the highly compressible Perdikas formation and the depression cone of the mine is present. The vertical displacements clearly decreased in the western part of the village with increasing distance from the mine.

The vertical displacement time series in the village of Valtonera shows a steadily decreasing trend with pronounced annual fluctuations. This observation is highly consistent with the water table time series at Valtonera village, which shows a steady downward trend with seasonal fluctuations. The observed trend of a continuous groundwater level drop can be attributed to the draining of the aquifer toward the mines, whereas the seasonal fluctuation likely results from exploitation of the aquifers for irrigation purposes followed by a partial rebound of the groundwater head during the winter [47]. As shown in Figure 8, the vertical displacements each year exhibit a decreasing trend until October (end of the dry period) followed by an increasing trend until May (end of the rainy period). Note that as this village was unaffected by the landslide (Figure S5), no abrupt scatter in the vertical and east–west displacement time series can be identified during the landslide period (Figure 8).

Considering the east–west horizontal displacement time series (Figure 7), most of the PSs around the village indicate a steady eastward displacement trend toward the open pit. These movements cannot be attributed to any landslide activity due to the great distance of the village from the mine (1800 m) relative to the height of the slopes (220 m). Thus, this deformation can only be attributed to ongoing land subsidence-driven deformation. It should be noted that the village is crossed by the Vegoritida fault (Fveg) dipping to the SE and that the fault acted as a pre-existing structural fabric that controls the orientation of the later ruptures generating slight horizontal movements.

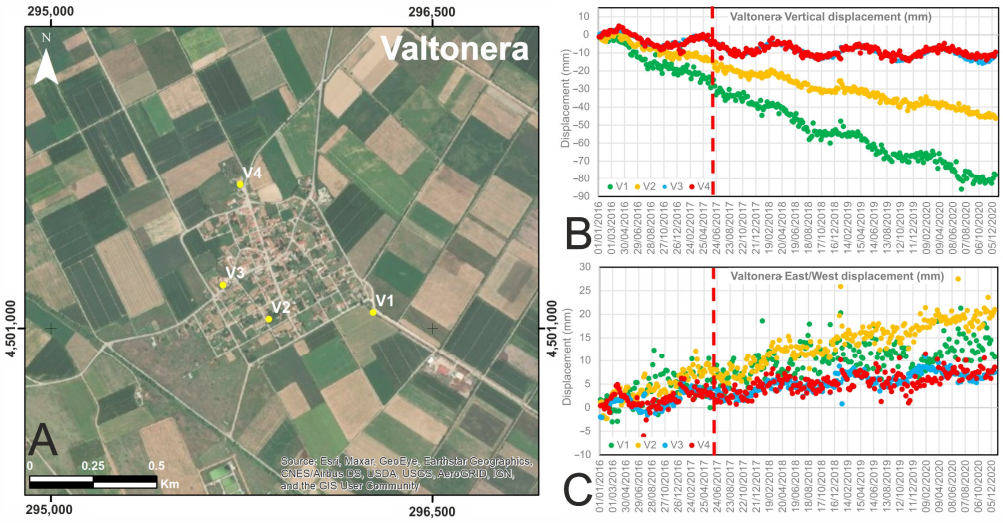

Figure 8. Spatial distribution of examined PS points (**A**) along with their displacement time series (**B**,**C**) at the village of Valtonera. The dashed line indicates the date of the mining landslide event.

The vertical displacements identified at the Fanos village are significantly less intense than those at the Valtonera and Anargiroi villages; nonetheless, this village also suffers from the occurrence of surface ruptures and differential deformation. These deformation types can be attributed to the pronounced stiffness and compressibility differences of the area's underlying formations, as the northern part of the village overlies Neogene rocks, and the western part overlies Quaternary formations.

Considering the vertical displacement time series (Figure 9), although annual fluctuations can be observed, there is no evidence of a gradually evolving long-term land subsidence trend. This implies that groundwater exploitation of the aquifer for irrigation needs is the main factor triggering the deformation that more strongly affects the softer and more compressible Quaternary formations. As shown in the deformation time series, no disturbance is recorded that can be attributed to the 10 June 2017 landslide (Figures 9 and S6); in addition, there are no clear trends observed in the east–west displacement values.

Figure 9. Spatial distribution of examined PS points (**A**) along with their displacement time series (**B**,**C**) at the village of Fanos. The dashed line indicates the date of the mining landslide event. The points were selected from both sides of the fault crossing the village, pointing to the displacements taking place on the stiff Neogene, point F1, and the soft Quaternary, point F2, formations.

5. Conclusions

In conclusion, the combination of ground truth data and information from EGMS datasets provides important insights into the mechanisms and interactions of geocatastrophic events taking place at the Amyntaio coal mine.

In particular, Anargiroi village is clearly affected by aquifer overexploitation via the mine's protection wells. The seasonal fluctuations in vertical deformation identified at Valtonera and Fanos villages, due to the operation of irrigation wells, are not visible in the vertical displacement time series acquired for Anargiroi village. Accordingly, farming activity is interpreted as not contributing significantly to land subsidence in the vicinity of Anargiroi village. This conclusion was largely expected as most of the farms in the village are irrigated from irrigation canals rather than from wells. In addition, the coincidence between the observed decreasing subsidence trends and the termination of pumping activities in 2016 between the open cast mine and the village also strongly supports the interpretation that the subsidence phenomenon is mainly caused by dewatering activities performed at the perimeter of the open cast mine. Regarding the effect of the 10 June 2017, landslide, the InSAR data set demonstrates that the failure affected and continues to affect at least the NE part of the village; in addition, slow horizontal movements toward the open pit are still taking place.

In terms of the deformation occurring at Valtonera village, the 10 June 2017, landslide did not affect the settlement due to the large distance between the village and the open cast mine. Subsidence in this area can be attributed to overpumping caused by both the mine's dewatering activity and farming activity. The mining activity appears to be responsible for the ongoing steady subsidence trend affecting the village, causing substantial damage. In contrast, farming activities in this area appear to cause gentle fluctuating deformations of a minor scale compared to those caused by mining activities.

The deformations at Fanos village are affected only by farming activity, as evidenced by the lack of any observed cross-seasonal or long-term deformation trend and the exclusive occurrence of seasonal deformation in this area. In addition, as expected, the fluctuating deformations appear to be more intense in areas of soft Quaternary formations rather than those of the stiff Neogene.

As a final conclusion, it should be stressed that EGMS datasets are a powerful resource for deciphering the different causal factors of deformations affecting the study area for more than two decades, highlighting the important role of the groundwater management. Because these datasets are provided by an independent and reliable international source, their conclusions are highly robust. Overall, InSAR techniques represent a highly important approach for the study of geohazards.

Supplementary Materials: The following supporting information can be downloaded at: https://www.mdpi.com/article/10.3390/w15081474/s1, Figure S1: The impact of land subsidence at the Anarigoi village. The photos were capture in May 2016 (before the landslide event that occurred on 10 June 2017); Figure S2: The impact of land subsidence at the Valtonera village. The photos were capture in May 2016 (before the landslide event that occurred on 10 June 2017); Figure S3: The impact of land subsidence at the Fanos village. The photos were capture in May 2016 (before the landslide event that occurred on 10 June 2017); Figure S4: The impact of landslide event in areas previously affected by land subsidence, at the Anarigoi village. The expansion of the surface raptures and the intensification of the damages on the constructions is clearly precented; Figure S5: Images taken at the Valtonera village before and after the occurrence of the major landslide event, that took place on 10 June 2017. It is clear that, as expected due to the large distance of the village from the open pit, the landslide did not cause any further damages to the already damaged, by the land subsidence, constructions of the village; Figure S6: Images taken at the Fanos village before and after the occurrence of the major landslide event, that took place on 10 June 2017. It is clear that, as expected due to the large distance of the village from the open pit, the landslide did not cause any further damages to the already damaged, by the land subsidence, constructions of the village; Figure S7: Images taken at the Anargyroi village after the occurrence of the major landslide event, that took place on 10 June 2017. The deformations taking place due to the continuous landslide and

land subsidence movements since the occurrence of the landslide are clearly presented; Table S1: Ground truth dataset.

Author Contributions: Methodology, P.T. and C.L.; Validation, P.T. and C.L.; Formal analysis, P.T.; Investigation, P.T.; Writing—original draft, P.T.; Writing—review & editing, C.L.; Supervision, C.L. All authors have read and agreed to the published version of the manuscript.

Funding: This research received no external funding.

Data Availability Statement: The datasets used and/or analyzed during the current study are available from the authors upon request.

Acknowledgments: The authors would like to acknowledge the European Land Monitoring Service of the European Environment Agency for freely providing the INSAR data.

Conflicts of Interest: The authors declare no conflict of interest.

References

1. Passariello, B.; Giuliano, V.; Quaresima, S.; Barbaro, M.; Caroli, S.; Forte, G.; Carelli, G.; Iavicoli, I. Evaluation of the environmental contamination at an abandoned mining site. *Microchem. J.* **2002**, *73*, 245–250. [CrossRef]
2. WISE_Uranium_Project. Chronology of Major Tailings Dam Failures. Available online: https://www.wise-uranium.org/mdaf.html (accessed on 30 August 2022).
3. Williams, C.; Ross, B.; Zebker, M.; Leighton, J.; Gaida, M.; Morkeh, J.; Robotham, M. Assessment of the available historic RADARSAT-2 synthetic aperture radar data prior to the manefay slide at the bingham canyon mine using modern InSAR techniques. *Rock Mech. Rock Eng.* **2021**, *54*, 3469–3489. [CrossRef]
4. Moore, J.R.; Pankow, K.L.; Ford, S.R.; Koper, K.D.; Hale, J.M.; Aaron, J.; Larsen, C.F. Dynamics of the Bingham Canyon rock avalanches (Utah, USA) resolved from topographic, seismic, and infrasound data. *J. Geophys. Res. Earth Surf.* **2017**, *122*, 615–640. [CrossRef]
5. Hibert, C.; Ekström, G.; Stark, C.P. Dynamics of the Bingham Canyon Mine landslides from seismic signal analysis. *Geophys. Res. Lett.* **2014**, *41*, 4535–4541. [CrossRef]
6. Pankow, K.L.; Moore, J.R.; Hale, J.M.; Koper, K.D.; Kubacki, T.; Whidden, K.M.; McCarter, M.K. Massive landslide at Utah copper mine generates wealth of geophysical data. *GSA Today* **2014**, *24*, 4–9. [CrossRef]
7. Lin, Y.N.; Park, E.; Wang, Y.; Quek, Y.P.; Lim, J.; Alcantara, E.; Loc, H.H. The 2020 Hpakant Jade Mine Disaster, Myanmar: A multi-sensor investigation for slope failure. *ISPRS J. Photogramm. Remote Sens.* **2021**, *177*, 291–305. [CrossRef]
8. Sun, Y.; Zhang, X.; Mao, W.; Xu, L. Mechanism and stability evaluation of goaf ground subsidence in the third mining area in Gong Changling District, China. *Arab. J. Geosci.* **2015**, *8*, 639–646. [CrossRef]
9. Carnec, C.; Delacourt, C. Three years of mining subsidence monitored by SAR interferometry, near Gardanne, France. *J. Appl. Geophys.* **2000**, *43*, 43–54. [CrossRef]
10. Wolkersdorfer, C.; Thiem, G. Ground water withdrawal and land subsidence in northeastern Saxony (Germany). *Mine Water Environ.* **1999**, *18*, 81–92. [CrossRef]
11. Tang, W.; Motagh, M.; Zhan, W. Monitoring active open-pit mine stability in the Rhenish coalfields of Germany using a coherence-based SBAS method. *Int. J. Appl. Earth Obs. Geoinf.* **2020**, *93*, 102217. [CrossRef]
12. Mohammady, M.; Pourghasemi, H.R.; Amiri, M. Assessment of land subsidence susceptibility in Semnan plain (Iran): A comparison of support vector machine and weights of evidence data mining algorithms. *Nat. Hazards* **2019**, *99*, 951–971. [CrossRef]
13. Hong, H.; Tsangaratos, P.; Ilia, I.; Loupasakis, C.; Wang, Y. Introducing a novel multi-layer perceptron network based on stochastic gradient descent optimized by a meta-heuristic algorithm for landslide susceptibility mapping. *Sci. Total Environ.* **2020**, *742*, 140549. [CrossRef]
14. Kaitantzian, A.; Loupasakis, C.; Tzampoglou, P.; Parcharidis, I. Ground Subsidence Triggered by the Overexploitation of Aquifers Affecting Urban Sites: The Case of Athens Coastal Zone along Faliro Bay (Greece). *Geofluids* **2020**, *2020*, 8896907. [CrossRef]
15. Svigkas, N.; Loupasakis, C.; Papoutsis, I.; Kontoes, C.; Alatza, S.; Tzampoglou, P.; Tolomei, C.; Spachos, T. InSAR Campaign Reveals Ongoing Displacement Trends at High Impact Sites of Thessaloniki and Chalkidiki, Greece. *Remote Sens.* **2020**, *12*, 2396. [CrossRef]
16. Nhu, V.-H.; Thi Ngo, P.-T.; Pham, T.D.; Dou, J.; Song, X.; Hoang, N.-D.; Tran, D.A.; Cao, D.P.; Aydilek, İ.B.; Amiri, M. A new hybrid firefly–PSO optimized random subspace tree intelligence for torrential rainfall-induced flash flood susceptible mapping. *Remote Sens.* **2020**, *12*, 2688. [CrossRef]
17. Ilia, I.; Tsangaratos, P.; Tzampoglou, P.; Chen, W.; Hong, H. Flash flood susceptibility mapping using stacking ensemble machine learning models. *Geocarto Int.* **2022**, *37*, 1–27. [CrossRef]
18. Tzampoglou, P.; Loukidis, D.; Koulermou, N. Seasonal Ground Movement Due to Swelling/Shrinkage of Nicosia Marl. *Remote Sens.* **2022**, *14*, 1440. [CrossRef]

19. Loupasakis, C. *Study of the Geotechnical Conditions of the Amintaio Coalmine Slopes Close to the Anargiri Village, Aetos Municipality, Florina Prefecture, Greece*; IGME: Athens, Greece, 2006; p. 48.
20. Tzampoglou, P.; Loupasakis, C. Updated ground water piezometry data of the Amyntaio sub-basin and their effect to the manifestation of the land subsidence phenomena. In Proceedings of the 11th International Hydorgeological Congress of Greece, Athens, Greece, 4–6 October 2017.
21. Loupasakis, C.; Angelitsa, V.; Rozos, D.; Spanou, N. Mining geohazards—Land subsidence caused by the dewatering of opencast coal mines: The case study of the Amyntaio coal mine, Florina, Greece. *Nat. Hazards* **2014**, *70*, 675–691. [CrossRef]
22. Tzampoglou, P.; Loupasakis, C. Mining geohazards susceptibility and risk mapping: The case of the Amyntaio open-pit coal mine, West Macedonia, Greece. *Environ. Earth Sci.* **2017**, *76*, 542. [CrossRef]
23. Tzampoglou, P.; Loupasakis, C. Evaluating geological and geotechnical data for the study of land subsidence phenomena at the perimeter of the Amyntaio coalmine, Greece. *Int. J. Min. Sci. Technol.* **2018**, *28*, 601–612. [CrossRef]
24. Loupasakis, C. Contradictive mining–Induced geocatastrophic events at open pit coal mines: The case of Amintaio coal mine, West Macedonia, Greece. *Arab. J. Geosci.* **2020**, *13*, 1–12. [CrossRef]
25. European Ground Motion Service. End-to-end Implementation and Operation of the European Ground Motion Service (EGMS). In *Product User Manual*; European Environment Agency (EEA): Copenhagen, Denmark, 2022.
26. European Union; European Environment Agency (EEA). Copernicus Land Monitoring Service. 2022. Available online: https://egms.land.copernicus.eu/ (accessed on 21 September 2022).
27. Crosetto, M.; Solari, L.; Mróz, M.; Balasis-Levinsen, J.; Casagli, N.; Frei, M.; Oyen, A.; Moldestad, D.A.; Bateson, L.; Guerrieri, L. The evolution of wide-area DInSAR: From regional and national services to the European Ground Motion Service. *Remote Sens.* **2020**, *12*, 2043. [CrossRef]
28. Crosetto, M.; Solari, L.; Balasis-Levinsen, J.; Bateson, L.; Casagli, N.; Frei, M.; Oyen, A.; Moldestad, D.; Mróz, M. Deformation monitoring at european scale: The copernicus ground motion service. *Int. Arch. Photogramm. Remote Sens. Spat. Inf. Sci.* **2021**, *XLIII-B3-2*, 141–146. [CrossRef]
29. Costantini, M.; Minati, F.; Trillo, F.; Ferretti, A.; Novali, F.; Passera, E.; Dehls, J.; Larsen, Y.; Marinkovic, P.; Eineder, M. European Ground Motion Service (EGMS). In Proceedings of the 2021 IEEE International Geoscience and Remote Sensing Symposium IGARSS, Brussels, Belgium, 11–16 July 2021; pp. 3293–3296.
30. Doukissa, K. *Geotechnical Study of the Bridge in the Central Trench of Aanargiroi Area*; Municipality of Aetos: Thessaloniki, Greece, 2010; p. 24.
31. Dhmaras, K.; Georgiadhs, M. *Lifting and Waterproofing Study of the Existing Embankment of Lake Cheimaditida Florina*; Geognosi Public Limited Company: Thessaloniki, Greece, 2002.
32. Tzampoglou, P. Mining geohazards in Greece. The case of the Amyntai open-pit coal mine. Ph.D. Thesis, National Technical University of Athens, Athens, Greece, 2017.
33. Koukouzas, C.; Kotis, T.; Ploumidis, M.; Metaxas, A. *Coal Exploration of Anargiri-Amynteon Area, Mineral Deposit Research*; Institution of Geology and Mineral Exploration: Athens, Greece, 1979; Volume 9.
34. Institution of Geology and Mineral Exploration. *Geological Map of Greece, Scale 1:50,000, Ptolemaida Sheet*; Institution of Geology and Mineral Exploration: Athens, Greece, 1997.
35. Metaxas, A.; Karageorgiou, D.; Varvarousis, G.; Kotis, T.; Ploumidis, M.; Papanikolaou, G. Geological evolution-stratigraphy of Florina, Ptolemaida, Kozani and Saradaporo graben. *Bull. Geol. Soc. Greece* **2007**, *40*, 161–172. [CrossRef]
36. Leonardos, M.; Terezopoulos, N. Rim slope failure mechanism in the Greek deep lignite mines–A case study. *Min. Technol.* **2003**, *112*, 197–204. [CrossRef]
37. Mountrakis, D. *Geology of Greece*; University Studio Press: Thessaloniki, Greece, 1985.
38. Spyropoulos, N. The geological structure of Pelagonian zone in the Mount of Askio D. Macedonia. Ph.D. Thesis, Aristotle University of Thessaloniki, Thessaloniki, Greece, 1992.
39. Pavlides, S.; Mountrakis, D. Neotectonics of the Florina-Vegoritis-Ptolemais Neogene Basin (NW Greece): An example of extensional tectonics of the greater Aegean area. *Ann. Géol. Pays Hell.* **1985**, *33*, 311–327.
40. Pavlides, S. Neotectonic evolution of the Florina-Vegoritis-Ptolemais basin (W. Macedonia, Greece). Ph.D. Thesis, Aristotle University of Thessaloniki, Thessaloniki, Greece, 1985.
41. Pavlides, S.; Mountrakis, D. Extensional tectonics of northwestern Macedonia, Greece, since the late Miocene. *J. Struct. Geol.* **1987**, *9*, 385–392. [CrossRef]
42. Koukouzas, C.; Kotis, T.; Ploumidis, M.; Metaxas, A.; Dimitriou, D. *Coal Exploration of Komninon-Ptolemaidas Area. Mineral Deposit Research*; Institution of Geology and Mineral Exploration: Athens, Greece, 1983; Volume 2.
43. Ganas, A.; Oikonomou, I.; Tsimi, A. NOAfaults: A digital database for active faults in Greece. *Bull. Geol. Soc. Greece* **2015**, *47*, 518–530. [CrossRef]
44. Stamos, A.; Giannoulopoulos, P. *Hydrogeological Report, Geotechnical Work to the Anargiri Village, Aetos Municipality, Florina Prefecture, Greece*; Institution of Geology and Mineral Exploration: Athens, Greece, 2010; p. 34.
45. Tzampoglou, P.; Loupasakis, C. New data regarding the ground water level changes at the Amyntaio basin-Florina Prefecture, Greece. *Bull. Geol. Soc. Greece* **2016**, *50*, 1006–1015. [CrossRef]
46. Tzampoglou, P.; Loupasakis, C. Land subsidence due to the overexploitation of the aquifer at the Valtonera village. *Bull. Geol. Soc. Greece* **2017**, *50*, 1006. [CrossRef]

47. Tzampoglou, P.; Loupasakis, C. Numerical simulation of the factors causing land subsidence due to overexploitation of the aquifer in the Amyntaio open coal mine, Greece. *HydroResearch* **2019**, *1*, 8–24. [CrossRef]
48. Dimitrakopoulos, D. Hydrogeological conditioning at the Amyndeon mine. Problems occuring during the exploitation and their mitigation actions. Ph.D. Thesis, NTUA, Athens, Greece, 2001.
49. Tsourlos, P. *Research for the Appearance of Surface Cracks in the Valtonera Village, Amyntaio Municipality, Florina Region*; School of Geology of the Aristotle University of Thessaloniki Aristotelian University of Thessaloniki: Thessaloniki, Greece, 2015; p. 17.
50. Soulios, G.; Tsapanos, T.; Voudouris, K.; Kaklis, T.; Mattas, C.; Sotiriadis, M. Ruptures on surface and buildings due to land subsidence in Anargyri village (Florina Prefecture, Macedonia). *Environ. Earth Sci.* **2011**, *5*, 505–512.
51. Dimitrakopoulos, D.; Koumantakis, I. Hydrodynamic regime of Amynteon basin. Influence of open lignite mines. In Proceedings of the 11th International Hydrogeological Congress of Greece, Athens, Greece, 4–6 October 2017; pp. 101–112.
52. Tzampoglou, P.; Loupasakis, C. Land subsidence susceptibility and hazard mapping: The case of Amyntaio Basin, Greece. In Proceedings of the Fifth International Conference on Remote Sensing and Geoinformation of the Environment (RSCy2017), Paphos, Cyprus, 20–23 March 2017; p. 104441L.
53. NOA. Earthquake Database Search. Available online: https://www.gein.noa.gr/en/services-products/database-search/ (accessed on 25 September 2022).